Oxygen off-stoichiometry and phase separation in EuO thin films

S. G. Altendorf,[1,2] A. Efimenko,[1,2] V. Oliana,[1,2] H. Kierspel,[1] A. D. Rata,[2] and L. H. Tjeng[2]
[1]*II. Physikalisches Institut, Universität zu Köln, Zülpicher Str. 77, DE-50937 Köln, Germany*
[2]*Max Planck Institute for Chemical Physics of Solids, Nöthnitzerstr. 40, DE-01187 Dresden, Germany*
(Received 19 July 2011; revised manuscript received 23 September 2011; published 28 October 2011)

We report on our study on the influence of the growth conditions on the europium/oxygen stoichiometry, morphology, magnetic properties, and electrical conductivity of EuO thin films. SQUID magnetometry and x-ray photoelectron spectroscopy were utilized as complementary techniques to determine the oxygen content of $EuO_{1\pm x}$ thin films grown by molecular beam epitaxy with and without the employment of the so-called Eu distillation process. We found indications for phase separation to occur in Eu-rich as well as in over-oxidized EuO for films grown at substrate temperatures below the Eu distillation temperature. Only a fraction of the excess Eu contributes to the metal-insulator transition in Eu-rich films grown under these conditions. We also observed that the surfaces of these films were ill defined and may even contain more Eu excess than the film average. Only EuO films grown under distillation conditions are guaranteed to have the same magnetic and electrical properties as stoichiometric bulk EuO, and to have surfaces with the proper Eu/O stoichiometry and electronic structure.

DOI: 10.1103/PhysRevB.84.155442 PACS number(s): 68.55.−a, 75.70.Ak, 79.60.−i, 81.15.Hi

I. INTRODUCTION

The rare-earth compound europium monoxide (EuO) is one of the few ferromagnetic semiconductors.[1] It has a Curie temperature of 69 K[2,3] and a room-temperature band gap of ≈1.12 eV.[4,5] The divalent Eu ions carry a large magnetic moment of $7\mu_B$ originating from the seven unpaired electrons in the atomic-like Eu $4f$ shell. In the ferromagnetic state, EuO exhibits very large magneto-optical effects, such as a Faraday rotation of 8.5×10^5 degree per cm at $\lambda = 0.7$ μm[6] and a Kerr rotation of 7.1° at $h\nu = 1.4$ eV.[7] Upon electron doping, the Curie temperature can be enhanced up to 125 K by incorporation of Gd.[8,9] It is even claimed that a Curie temperature of 200 K can be reached by using La.[10] In Eu-rich EuO, a metal-insulator transition (MIT) occurs upon cooling, accompanied by a colossal magnetoresistance with unprecedented changes in resistivity exceeding 8–13 orders of magnitude.[11,12]

In the last decade, the research on EuO was especially driven by the strong interest from the field of spintronics.[8–10,13–47] This attention was triggered by the expectation that the charge carriers in doped EuO should have a nearly 100% spin polarization associated with the spin splitting of the bottom of the conduction band of about 0.6 eV in the ferromagnetic state.[18] In subsequent studies, it was shown that the deposition of EuO films can be made compatible with the Si technology. A preservation of 90% spin polarization for epitaxial[26] as well as for polycrystalline[30] EuO films demonstrates its potential as device material for an efficient spin injection.

It is very surprising that the issue of oxygen stoichiometry in EuO thin films[8–10,13–46] is hardly addressed. This might be caused by the fact that standard experimental methods such as thermogravimetric analysis (TGA), energy-dispersive x-ray spectroscopy (EDX), and chemical titration are not compatible for this particular system. The absolute amount of material to be analyzed is extremely small for thin films and EuO is highly air sensitive prohibiting the direct application of *ex situ* methods, i.e., special capping layers need to be designed first. To the best of our knowledge, there is only one study reporting on the determination of the oxygen stoichiometry. This work uses polarized neutron reflectometry on polycrystalline thin films containing a complex mixture of EuO_{1-x} ($x = 2.5 - 9\%$), Eu metal (7–16%), and Eu_2O_3 (10–14%).[47] Here, we report on our work to determine the concentration of oxygen vacancies in EuO_{1-x} thin films starting from a single crystalline stoichiometric EuO. Hereby, we aim to carefully avoid the presence of Eu_2O_3 while investigating the Eu-rich part of the EuO phase diagram in order to obtain a more direct view on the influence of the oxygen defects. We use x-ray photoelectron spectroscopy (XPS) whose probing sensitivity makes this technique ideal for thin films and surfaces. Furthermore, we utilize an experimental setup that allows for the preparation, structural characterization, spectroscopic analysis, and measurement of the resistivity to be done all *in situ* providing a high reliability and reproducibility of the results. We also carried out complementary *ex situ* magnetization measurements on properly capped thin films. Our objective is to establish the relationship between stoichiometry, morphology, electronic structure, and properties of these doped EuO films.

II. EXPERIMENT

The EuO films were prepared by molecular beam epitaxy under ultrahigh vacuum conditions with base pressures in the range of 1×10^{-10} mbar. High-purity Eu metal was evaporated from an effusion cell at temperatures of about 415 °C in a molecular oxygen atmosphere. The Eu flux rate was calibrated using a quartz-crystal thickness monitor at the growth position prior to deposition and set to 8.1 ± 0.1 Å/min for all films. Extensive degassing of the Eu material ensured a pressure below 2×10^{-9} mbar (mainly hydrogen) during Eu evaporation. Molecular oxygen was supplied through a leak valve placed far away from the growth position. The partial oxygen pressure was varied between 3.5 and 7.0×10^{-8} mbar above the background pressure and was monitored using an ion gauge and a quadrupole mass spectrometer. The growth was terminated after 90 min by simultaneously closing the oxygen leak valve and Eu shutter.

 ©2011 American Physical Society

Epi-polished yttria-stabilized cubic zirconia (YSZ) (001) single crystals were chosen as substrates. With a lattice constant of about 5.142 Å,[48] this substrate matches almost perfectly the rock-salt structure of EuO with a = 5.144 Å;[49] and it was shown by Sutarto *et al.* that EuO films can be grown epitaxially in a smooth layer-by-layer fashion on YSZ (001) with perfect stoichiometry and proper magnetic properties.[36] Furthermore, the large band gap of >4 eV (see Ref. 50) facilitates reliable resistivity measurements on the highly insulating EuO films. Prior to EuO deposition, the substrates were annealed at 600 °C in an oxygen atmosphere of 1×10^{-7} mbar for at least 2 hours to achieve clean and well-ordered surfaces.

The crystalline growth of the films was verified during deposition using an EK-35-R reflection high-energy electron diffraction (RHEED) system from STAIB Instruments. The crystalline structure was also studied after growth by low-energy electron diffraction (LEED) using a Vacuum Generators Scientific T191 rear-view system. The photoemission spectra were recorded in a spectrometer equipped with a Vacuum Generators twin crystal monochromatized Al-K_α source ($h\nu = 1486.6$ eV) and a Scienta electron energy analyzer R3000. The overall resolution was set to ≈0.4 eV. The x-ray photoelectron spectroscopy (XPS) data were collected at normal emission geometry and at room temperature unless stated otherwise. The temperature-dependent transport measurements were performed *in situ* in a standard two-point arrangement. Before EuO deposition, two chromium electrodes (thickness ≈ 50 nm, width = 2 mm, gap = 40 μm) were deposited *ex situ* on the YSZ substrates. A voltage of 9 V was supplied by a conventional battery, and the induced current was measured using a Keithley model 6512 electrometer. In this way, resistances up to about 1×10^{13} Ω could be measured reliably. The magnetic properties of the EuO films were investigated *ex situ* in a Quantum Design MPMS-XL7 superconducting quantum interference device (SQUID) magnetometer. To protect the sensitive samples against degradation in air, they were capped with an aluminum film of about 50 Å thickness.

III. RESULTS A: CONSTANT SUBSTRATE TEMPERATURE, VARYING OXYGEN PRESSURES

We start first with a series of $EuO_{1\pm x}$ samples in which the substrate temperature during growth is fixed at 200 °C and the oxygen pressure is varied between 3.5 and 7.0×10^{-8} mbar. The Eu rate is set at 8.1 ± 0.1 Å/min for all samples.

The crystallinity of the EuO films was investigated by electron diffraction experiments. In Fig. 1, the RHEED and LEED images for the different oxygen pressures are shown. The RHEED electron energy was set to 20 keV with the incident beam aligned parallel to the [100] direction of the substrate. The LEED patterns were taken at electron energies of about 150 eV. The best surface structure was observed for the sample grown at 5.5×10^{-8} mbar oxygen pressure. The sharp RHEED streaks and intense LEED spots indicate a flat and well-ordered (001) fcc surface structure of EuO. The distances of the LEED spots and RHEED streaks of the EuO film are identical to those of YSZ confirming closely matching in-plane lattice constants of film and substrate. For low oxygen pressures, the LEED spots are broadened and less intense and the RHEED patterns become blurry indicating an increasing disorder in the films. For pressures only slightly above $P_{ox} = 5.5\times10^{-8}$ mbar, the patterns get rapidly worse. The RHEED photographs show a weak polycrystalline ring structure and the LEED pattern even vanishes completely suggesting considerable surface roughness and loss of crystallinity.

To check the Eu valence, we measured the valence band spectra of the $EuO_{1\pm x}$ films using XPS. The results are displayed in Fig. 2. For comparison, the spectrum of a Eu metal film is also included. The line shape of the Eu $4f$ peak at 2 eV binding energy of the films grown at oxygen pressures in the range of 3.5 to 5.5×10^{-8} mbar is characteristic for Eu^{2+}. For the $EuO_{1\pm x}$ films, one can also observe the oxygen $2p$ band, which is located between 4 and 6 eV. For the samples grown at $P_{ox} = 6.0$–7.0×10^{-8} mbar, a broad feature between 6 and 12 eV appears. This is characteristic for Eu^{3+}. Obviously, these samples consist of a mixture of EuO and Eu_3O_4 or Eu_2O_3 phases. Based on the photoemission results, we can infer a maximum oxygen pressure for the EuO growth of about 5.5

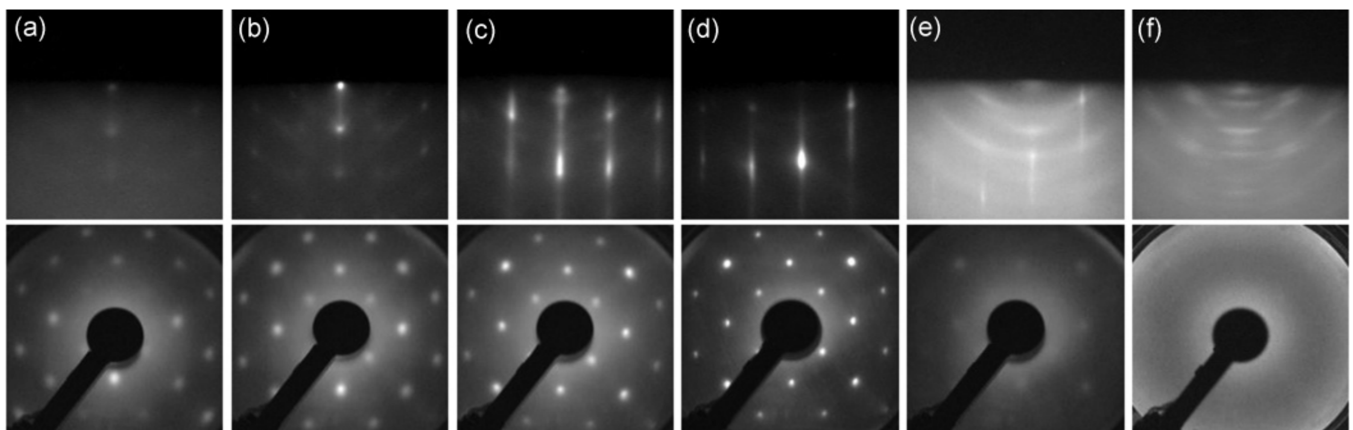

FIG. 1. Electron diffraction images of $EuO_{1\pm x}$ films on YSZ (001) grown for 90 min at $T_{substrate} = 200$ °C and $\Phi_{Eu} = 8.1 \pm 0.1$ Å/min. The oxygen pressure was set to (from left to right) (a) 3.5, (b) 4.0, (c) 5.0, (d) 5.5, (e) 6.0, and (f) 7.0×10^{-8} mbar. Top panels: RHEED patterns taken at 20 keV electron energy. The electron beam was aligned parallel to the [100] direction. Bottom panels: corresponding LEED patterns recorded at electron energies of about 150 eV.

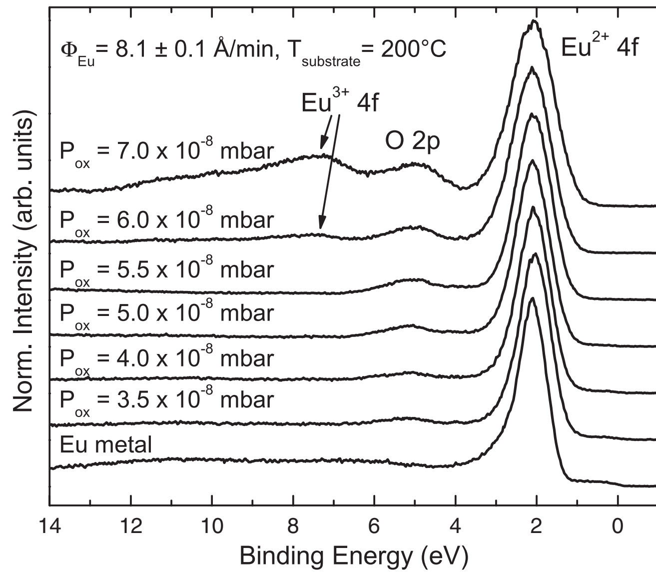

FIG. 2. Eu $4f$ and O $2p$ valence band XPS spectra of $EuO_{1\pm x}$ films on YSZ (001). All films were grown at 200 °C substrate temperature with a Eu flux rate of 8.1 ± 0.1 Å/min for 90 min. The supplied oxygen pressure was varied between 3.5 and 7.0 × 10^{-8} mbar (from bottom to top).

to 6.0 × 10^{-8} mbar for a Eu rate of 8.1 Å/min. Keeping the oxygen pressure during deposition below this maximum value, EuO can be grown without any contamination of Eu^{3+} species.

Figure 3 displays the resistivity of the samples and its temperature dependence. We observe that the higher the oxygen pressure, the higher the resistivity is. For the highest oxygen pressures, namely 7.0 and 6.0 ×10^{-8} mbar, the samples are insulating. Cooling down below 200 K, the resistivity of these samples exceeds the maximum limit of our setup. The samples grown at lower oxygen pressures of 3.5 to 5.5 × 10^{-8} mbar also show a semiconducting behavior at high temperatures. However, at temperatures of around 60–75 K a transition to a metallic phase occurs. The resistivity then drops by about two to four orders of magnitude in going to low

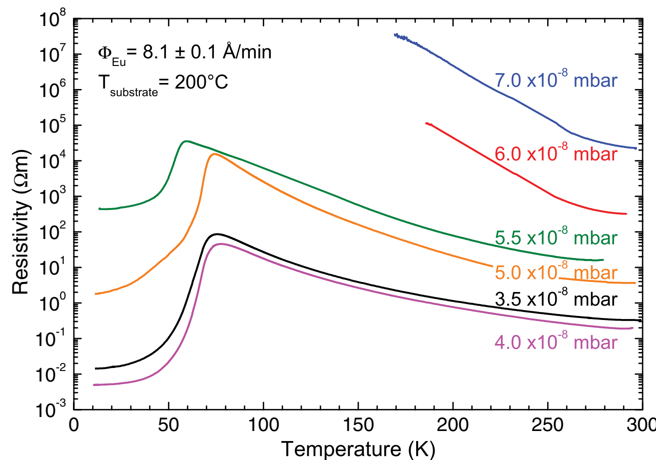

FIG. 3. (Color online) Temperature-dependent resistivity of $EuO_{1\pm x}$ samples grown at 200 °C substrate temperature for various oxygen pressures.

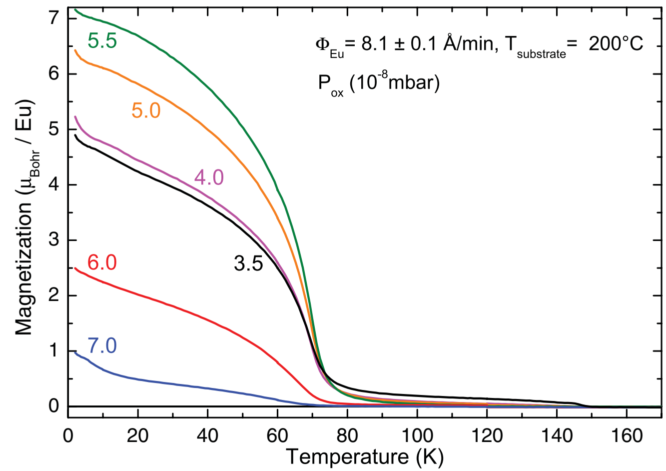

FIG. 4. (Color online) Temperature dependence of the magnetization of $EuO_{1\pm x}$ films on YSZ (001) grown at 3.5–7.0×10^{-8} mbar oxygen pressure. The applied magnetic field was 1000 G. The magnetic moment was calculated by assuming the same Eu amount for all films.

temperatures.[51] Similar MIT phenomena have been observed in EuO thin film studies that have reported the temperature dependence of the resistivity.[9,17,18,20,26,52] It is known for bulk EuO that an MIT only occurs for oxygen-deficient samples, suggesting the possibility that the MIT in EuO thin films is also associated with the presence of oxygen vacancies.

To investigate the magnetic properties of these EuO thin films, SQUID measurements were performed. The results of the temperature-dependent magnetization measurements for an applied magnetic field of 1000 G are depicted in Fig. 4. The magnetization is plotted assuming the same Eu amount for all films, since all films have been grown for the same amount of time and the same Eu evaporation rate. We find that the magnetization increases with oxygen pressure to a maximum value for the sample grown at P_{ox} = 5.5×10^{-8} mbar. The magnetization curves of these films mainly follow the Brillouin function with Curie temperature of 69 K. A further increase of the oxygen pressure leads to a significant reduction of the magnetization. The magnetization of the sample grown at P_{ox} = 6.0×10^{-8} mbar is reduced by a factor of three and for the sample grown at P_{ox} = 7.0×10^{-8} mbar by a factor of seven compared to the sample grown at P_{ox} = 5.5×10^{-8} mbar. Remarkably, the shapes of the magnetization curves are still very similar to that of EuO, suggesting that these two high-pressure films still contain some ferromagnetic EuO regions in addition to Eu^{3+} oxide species as revealed by the XPS measurements.

It is important to note that the samples grown under low oxygen pressure conditions show a long magnetization tail above the EuO Curie temperature. This tail can go up as high as 150 K. This enhancement of the Curie temperature was also observed in several Eu-rich EuO thin film studies.[20,47,52–56] To unravel the origin of this tail, we have carried out the magnetization measurements for different applied magnetic fields. Figure 5 displays the results of the measurements performed at 10, 100, and 1000 G for the sample grown at P_{ox} = 3.5× 10^{-8} mbar. We found that the nonzero magnetization above the EuO Curie temperature is only observed for measurements

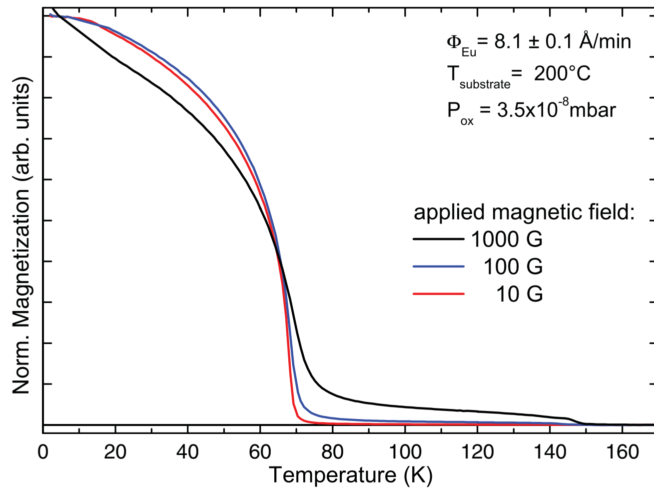

FIG. 5. (Color online) Normalized temperature-dependent magnetization curves of the EuO film grown at 3.5×10^{-8} mbar oxygen, 200 °C substrate temperature and Eu flux rate of 8.1 ± 0.1 Å/min on YSZ (001) measured at applied magnetic fields of 10, 100, and 1000 G.

performed at high magnetic fields and that it is increasing with rising fields. This behavior can be taken as an indication for the presence of Eu metal clusters in the doped samples that align when high magnetic fields are applied.

From the magnetization curves, we can also extract an estimation of the effective EuO content of the films. The results are shown in Fig. 6. For oxygen pressures of 3.5 to 5.5×10^{-8} mbar, the EuO content is increasing proportionally to the oxygen pressure. The sample grown at $P_{ox} = 5.5\times10^{-8}$ mbar with the highest magnetization is assumed to be close to stoichiometric. Thus, its effective EuO content is set to 100%. We then observe that for higher oxygen pressures when Eu^{3+} is formed, the EuO content is significantly reduced to about 35% of the maximum value for $P_{ox} = 6.0\times10^{-8}$ mbar and to about 10% for $P_{ox} = 7.0\times10^{-8}$ mbar. Stoichiometric EuO can be found at pressures of around 5.5 to 6.0×10^{-8} mbar for the given Eu evaporation

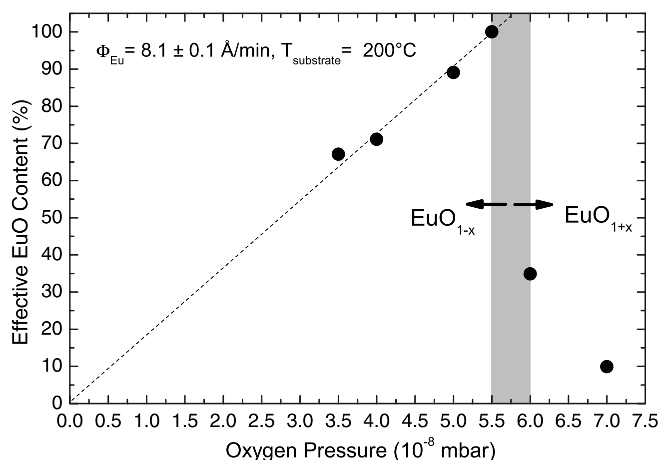

FIG. 6. Effective EuO content of the $EuO_{1\pm x}$ films grown at 200 °C for different oxygen pressures as determined from the magnetization measurements. The value of the highest EuO content for the sample grown at $P_{ox} = 5.5\times10^{-8}$ mbar is set to 100%.

rate of 8.1 Å/min. The grey area in Fig. 6 forms the boundary between Eu-rich EuO and over-oxidized EuO. We thus find out that the films showing MIT as displayed in Fig. 3 could have oxygen deficiencies as much as several tens of percents. It is conceivable that the very large amount of oxygen vacancies will not be homogeneously distributed in the material and that instead a phase separation may occur in which regions of EuO coexist with Eu metal clusters as we have already inferred from the magnetic field dependence of the magnetization tail, see Fig. 5. Perhaps this may also explain why the MIT is rather broad in temperature.

IV. RESULTS B: CONSTANT OXYGEN PRESSURE, VARYING SUBSTRATE TEMPERATURES

A second series of EuO samples was grown under a fixed oxygen pressure of 5.0×10^{-8} mbar but for temperatures varying between 200 and 300 °C. The Eu rate is still set at 8.1 Å/min, so we will be in the Eu-rich EuO part of the EuO phase diagram. Using this procedure we expect to have films with the same amount of EuO across the series, since the amount of oxygen supplied is the same. Yet, we expect to have a variation of the amount of Eu excess related to the fact that the reevaporation of the Eu excess from the sample surface depends strongly on the temperature of the substrate.

Figure 7 shows the RHEED and LEED images of the films prepared in this manner. All samples exhibit a good crystalline structure as indicated by the bright sharp diffraction patterns. The LEED photographs were taken at electron energies of about 220 eV. They show an improving surface crystallinity for temperatures up to 270 °C as indicated by the decreasing background intensity. For higher substrate temperatures of 280 and 300 °C, the background intensity is enhanced, which can be ascribed to charging effects owing to the high resistivity of the films.

The XPS valence band spectra, depicted in Fig. 8, verify that all films are purely Eu^{2+}. No indication for any Eu^{3+} contamination was observed as expected.

Also for this set of samples, *in situ* transport measurements were performed as displayed in Fig. 9. All samples show semiconducting behavior at high temperatures with higher room-temperature resistivity for the samples grown at high substrate temperature indicating a decreasing Eu excess. While the samples grown at 270 to 300 °C substrate temperatures are semiconducting for all temperatures, the samples grown at lower temperatures exhibit an MIT at around the magnetic transition with resistivity changes up to five orders of magnitude. The data suggest that the high-temperature samples are close to stoichiometric EuO whereas the low-temperature films have non-negligible Eu excess.

The SQUID measurements, displayed in Fig. 10, show that all samples have the typical Brillouin-like magnetization curves. Also here there is a tail above the EuO Curie temperature for applied magnetic fields of 1000 G. Nevertheless, this tail going up to 150 K is much smaller in this series than for the samples grown under lower oxygen pressure conditions, see Fig. 4. This indicates that the present set of samples has better EuO stoichiometry. In plotting Fig. 10 we have normalized the magnetization curves to their 5 K value. Yet, from the absolute value of the magnetization data we can extract the effective film

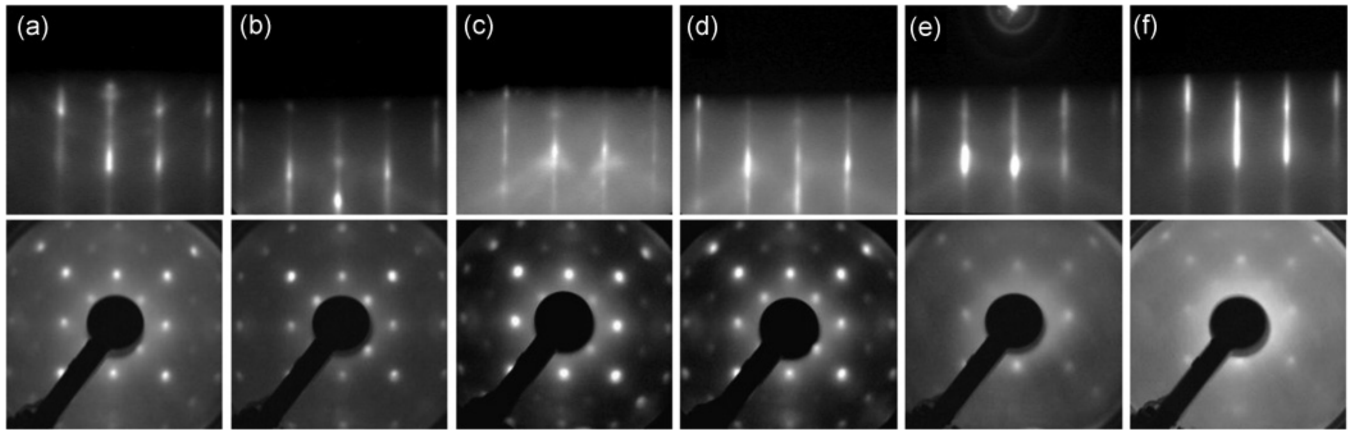

FIG. 7. Electron diffraction images of EuO_{1-x} films on YSZ (001) grown for 90 min at $P_{ox} = 5.0 \times 10^{-8}$ mbar and $\Phi_{Eu} = 8.1 \pm 0.1$ Å/min. The substrate temperature was set to (from left to right) (a) 200, (b) 250, (c) 260, (d) 270, (e) 280, and (f) 300 °C. Top panels: RHEED patterns taken at 20 keV electron energy. The electron beam was aligned parallel to the [100] direction. Bottom panels: corresponding LEED patterns recorded at electron energies of about 220 eV.

thickness of the EuO part. These values are plotted in Fig. 11. One can clearly see that the values are nearly constant, varying a little between 52 and 59 nm over the series. This confirms that the distillation process does indeed not change the amount of EuO in our samples but only the amount of Eu excess.

V. RESULTS C: XPS CHARACTERIZATION OF OXYGEN VACANCIES

To determine the oxygen content of our $EuO_{1\pm x}$ thin films, we have performed XPS measurements focusing on the O 1*s* and Eu 4*d* core levels. We start with the second series of samples in which we varied the substrate temperature during growth, but kept the oxygen pressure fixed at 5.0×10^{-8} mbar.

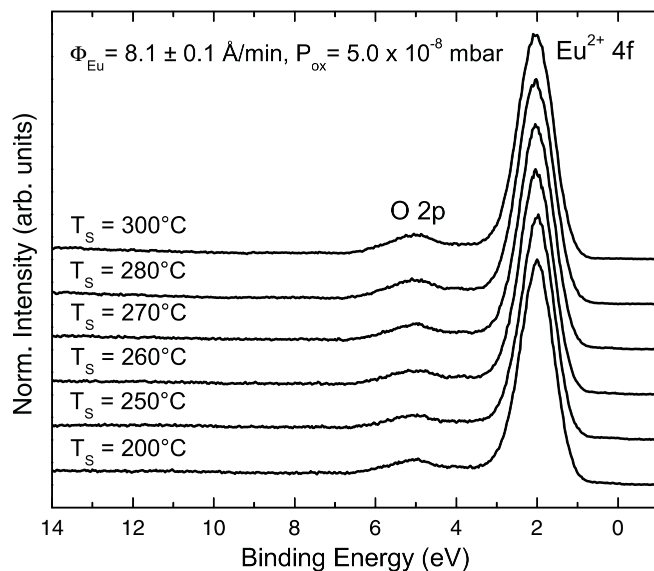

FIG. 8. Eu 4*f* and O 2*p* valence band XPS spectra of EuO_{1-x} films on YSZ (001). All films were grown at $P_{ox} = 5.0 \times 10^{-8}$ mbar with a Eu flux rate of 8.1 ± 0.1 Å/min for 90 min. The substrate temperature was varied between 200 and 300 °C (from bottom to top).

The XPS results are shown in Fig. 12. The intensity of the O 1*s* peak is increasing for substrate temperatures above 250 °C. This is consistent with our expectation that the higher the substrate temperature the more excess Eu is reevaporated resulting in an increasing oxygen content in the films. To obtain a quantitative number for the O/Eu ratio, we compare the integrated intensities of the O 1*s* and Eu 4*d* peaks. The results for the different oxygen pressures are plotted in Fig. 13.

The constant O/Eu ratio of about 0.17 for the samples grown at 200 and 250 °C reveals that at these relatively low substrate temperatures, no Eu distillation process takes place.[17,23,36] For temperatures above 250 °C, the O/Eu ratio increases steadily to a value of 0.23 for the sample grown at 280 °C. For a substrate temperature of 300 °C, the increase of the O/Eu ratio starts to saturate indicating that at this temperature almost all Eu excess is distilled. Thus we can conclude that the value for the O/Eu ratio of stoichiometric EuO is about 0.25.

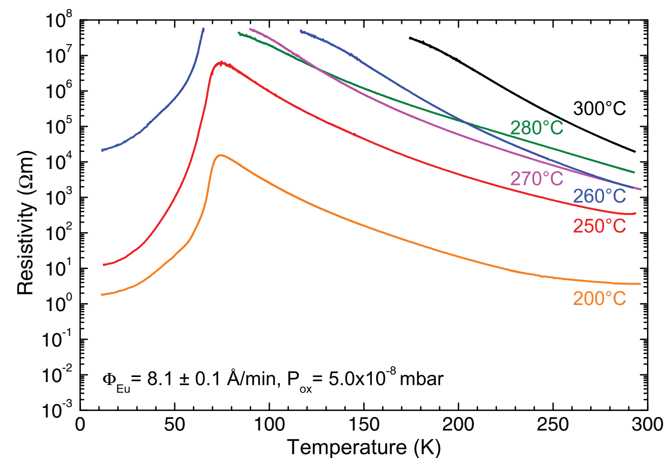

FIG. 9. (Color online) Temperature-dependent resistivity of EuO_{1-x} samples grown at $P_{ox} = 5.0 \times 10^{-8}$ mbar for substrate temperatures of 200–300 °C.

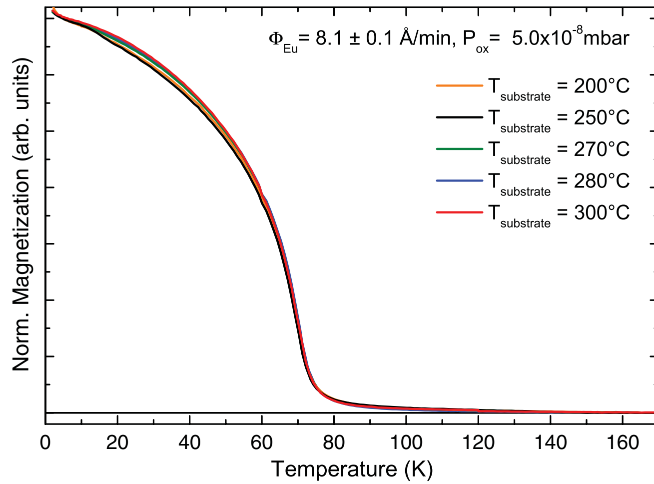

FIG. 10. (Color online) Temperature-dependent magnetization of EuO_{1-x} films on YSZ (001) grown at various substrate temperatures. The spectra are normalized at the 5 K value. The applied magnetic field was 1000 G.

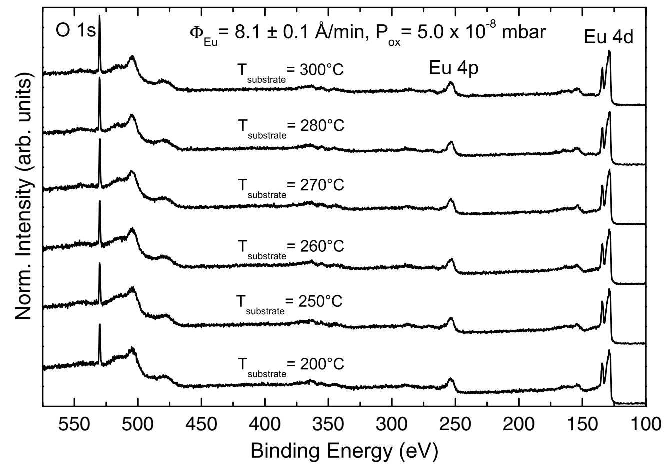

FIG. 12. O 1s and Eu 4d core-level XPS spectra of EuO_{1-x} films on YSZ (001). All films were grown at 5.0×10^{-8} mbar oxygen pressure with a Eu flux rate of 8.1 ± 0.1 Å/min for 90 min. The substrate temperature was varied between 200 and 300 °C (from bottom to top).

Figure 14 shows a close up of the Fermi-level region of the room-temperature XPS spectra to investigate in more detail the spectral features of the valence band in the vicinity of the chemical potential. For the samples grown at 280 and 300 °C, no spectral weight at the Fermi level can be detected, whereas the samples prepared at low substrate temperatures feature clearly a Fermi cutoff. Important is that this metallic feature extends from the Fermi level all the way to the Eu 4f region, which is characteristic for metallic Eu. This can be taken as an indication that the excess Eu indeed forms metal clusters. We do not observe a clear sign for the formation of impurity bands, in which case one would expect to see a narrow band around the Fermi level well separated from the Eu 4f.

To address this issue further, we study the nature of the metallic state of the system by looking at the temperature dependence of the Fermi-level region. For the sample grown at 260 °C, the valence band was measured at 20 and 130 K, well below and well above the metal-insulator transition, respectively. Figure 15 shows that the spectral weight hardly changes across the MIT. This suggests that the amount of doped electrons that cause the MIT must be much smaller compared to the total amount of excess Eu, i.e., that there are only few oxygen defects present that can release electrons at low temperatures, which is in accordance with theoretical models.[59,60] This in turn is consistent with the picture that most of the excess Eu forms clusters.

Now we focus on the O/Eu ratio of the first series of $EuO_{1\pm x}$ samples grown at 200 °C substrate temperature under varying oxygen pressure. The O 1s and Eu 4d core level XPS spectra are shown in Fig. 16. One can clearly observe that the intensity of the O 1s peak is increasing with increasing oxygen pressure indicating that the oxygen content of the films depends directly on the supplied oxygen. No excess Eu is distilled in this growth process. The Eu 4d peak again confirms the formation of Eu^{3+} for $P_{ox} \geqslant 6.0 \times 10^{-8}$ mbar. The line shape starts then to change

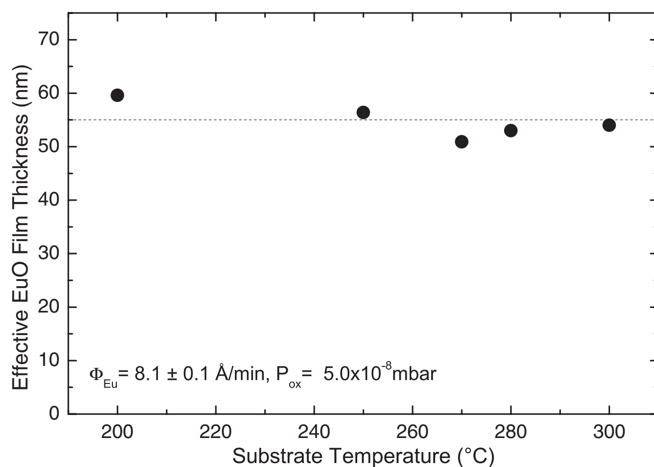

FIG. 11. Effective EuO film thickness as calculated from the SQUID results by assuming a magnetic moment of 7μ_B per Eu for EuO films grown at substrate temperatures of 200–300 °C.

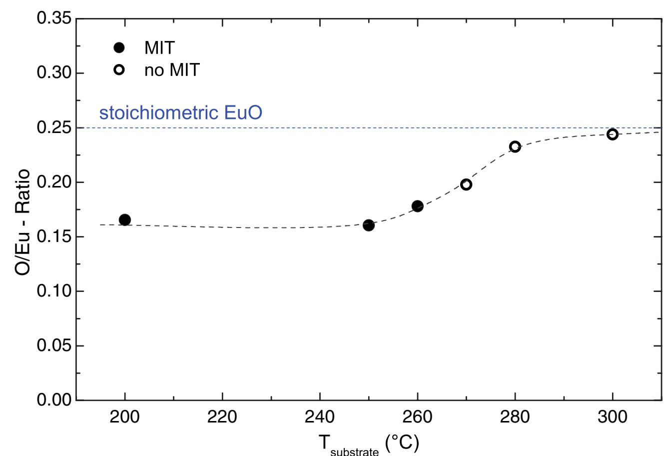

FIG. 13. (Color online) O/Eu ratio of EuO_{1-x} films on YSZ (001) grown at $P_{ox} = 5.0 \times 10^{-8}$ mbar at substrate temperatures of 200–300 °C as determined from the integrated O 1s/Eu 4d XPS intensities.

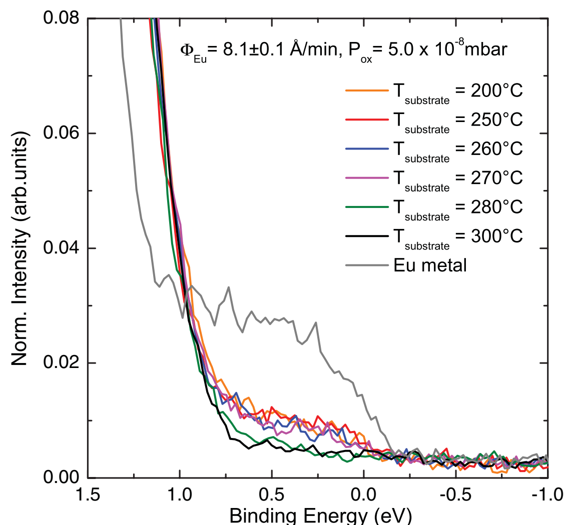

FIG. 14. (Color online) Fermi-level region of the photoemission spectra of the EuO_{1-x} films grown at $P_{ox} = 5.0 \times 10^{-8}$ mbar for various substrate temperatures. The spectra were collected at room temperature. For comparison, also the spectrum of a Eu metal film is shown.

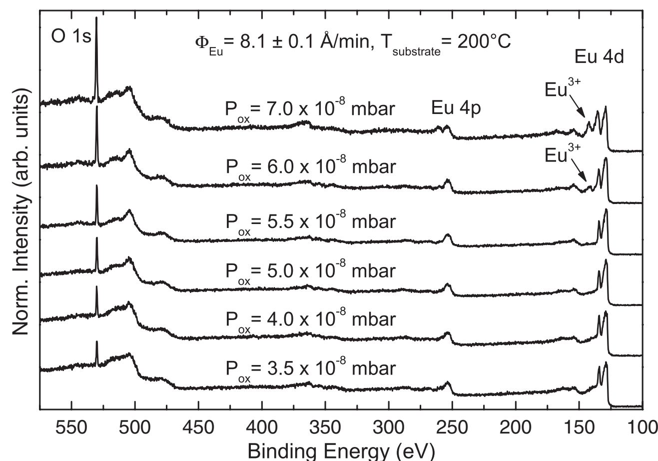

FIG. 16. O 1*s* and Eu 4*d* core-level XPS spectra of $EuO_{1\pm x}$ films on YSZ (001). All films were grown at 200 °C substrate temperature with a Eu flux rate of 8.1 ± 0.1 Å/min for 90 min. The supplied oxygen pressure was varied between 3.5–7.0$\times 10^{-8}$ mbar (from bottom to top).

and a characteristic feature of Eu^{3+} at 142 eV binding energy comes up.

The extracted O/Eu ratio is displayed in Fig. 17. For the Eu-rich samples grown at $P_{ox} \leqslant 5.5\times10^{-8}$ mbar, the O/Eu ratio increases linearly with the oxygen pressure from 0.09 to 0.20. For higher oxygen pressures when Eu^{3+} starts to form, the values jump to 0.29 and 0.32. From the results of the second series of EuO samples, we already know that stoichiometric EuO has an O/Eu ratio of 0.25, cf. Fig. 13. Furthermore, from the magnetization measurements, we know that stoichiometric EuO can be grown at an oxygen pressure of about 5.5 to 6.0×10^{-8} mbar for a substrate temperature of 200 °C, see Fig. 4. With these numbers and the assumption that the O/Eu ratio is proportional to the oxygen pressure, we can draw a line for the expected course of the O/Eu ratio curve. Obviously, the XPS values for the O/Eu ratios for the Eu-rich samples lie all appreciably below the expected values, meaning that samples seem to contain more Eu than expected. The effective EuO content extracted from the magnetization measurements, see Fig. 6, however, behaves proportionally with oxygen pressure. Thus, it is conceivable that the observed deviation of the XPS analysis could be related to the surface of the samples, since XPS is a very surface-sensitive technique with probing depths of about 10–15 Å. The stoichiometry of the surface of the Eu-rich EuO samples is apparently different from that of the bulk. It seems that for the Eu-rich EuO samples there is an extra excess of Eu at the surface.

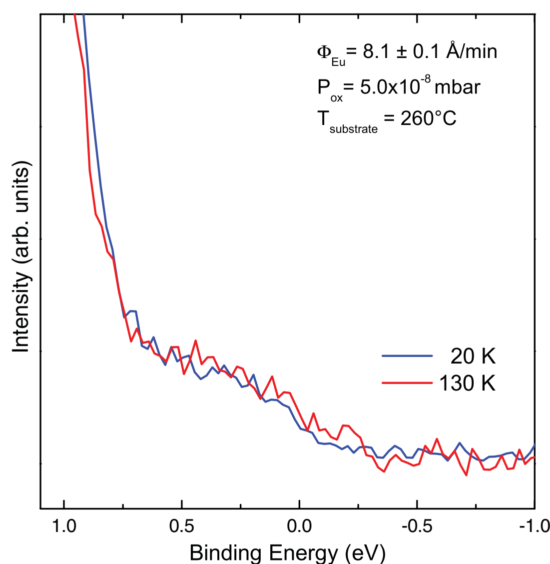

FIG. 15. (Color online) Fermi-level region of the photoemission spectra of the EuO_{1-x} film grown at $P_{ox} = 5.0 \times 10^{-8}$ mbar, a Eu rate of 8.1 ± 0.1 Å/min and substrate temperature of 260 °C. The spectra were collected at 20 and 130 K.

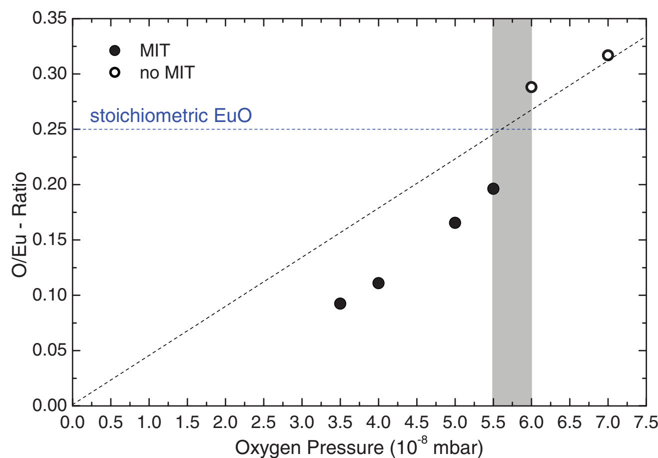

FIG. 17. (Color online) O/Eu ratio of $EuO_{1\pm x}$ films on YSZ (001) grown at 200 °C substrate temperature for $P_{ox} = 3.5$–7.0×10^{-8} mbar as determined from the integrated O 1*s*/Eu 4*d* XPS intensities.

VI. CONCLUSIONS

We have carried out a comprehensive study on the influence of the growth conditions on the properties of EuO thin films. We have utilized molecular beam epitaxy on YSZ (001) substrates, with and without the application of the so-called Eu distillation process. The films were characterized using *in situ* RHEED and LEED electron diffraction techniques, *in situ* x-ray photoelectron spectroscopy, and *in situ* temperature-dependent resistivity measurements. *Ex situ* SQUID magnetometry was used on aluminum-capped films to characterize their magnetic properties.

From the magnetization and x-ray photoemission experiments, we found indications that phase separation occurs in Eu-rich as well as in over-oxidized EuO for films grown at substrate temperatures below the Eu distillation temperature. From the lack of any noticeable changes in the metallic features of the valence band across the metal-insulator transition, we conclude that only a fraction of the excess Eu contributes to the metal-insulator transition in Eu-rich films grown under these conditions. We also observed that the surfaces of these films were ill defined and may even contain more Eu excess than the film average. However, the RHEED and LEED may still display the (001) diffraction pattern, despite the fact that up to several tens of percents of oxygen is lacking in the films. It is therefore tempting to speculate that the Eu metal clusters may even have the fcc structure with a quite similar lattice constant as the EuO, effectively giving us the equivalent picture that the large amounts of oxygen vacancies in Eu-rich EuO films condense and form clusters. We note that the existence of fcc Eu may not be too unrealistic since it has been claimed earlier in the literature that Eu metal films could have the fcc structure if grown on particular metal substrates.[57,58]

Important is that the films grown under Eu distillation conditions always yield stoichiometric EuO with the proper properties, namely semiconducting over all temperature ranges and ferromagnetic with a 69 K Curie temperature and a $7\mu_B$ magnetic moment. The surfaces of these films have also the proper Eu/O stoichiometry and electronic structure. Yet, it is close to impossible to carry out low-temperature photoemission measurements on these type of films due to the severe charging problems associated with their highly insulating nature. Films measured at low temperatures must therefore necessarily contain defects or dopants.

ACKNOWLEDGMENTS

We would like to thank Lucie Hamdan and Susanne Heijligen for their skillful technical assistance. The research in Cologne is supported by the Deutsche Forschungsgemeinschaft through SFB 608. A.E. is also supported by the EU through the Marie Curie (FP7) ITN SOPRANO project.

[1] B. T. Matthias, R. M. Bozorth, and J. H. Van Vleck, Phys. Rev. Lett. **7**, 160 (1961).

[2] E. L. Boyd, Phys. Rev. **145**, 174 (1966).

[3] A. Kornblit and G. Ahlers, Phys. Rev. B **11**, 2678 (1975).

[4] G. Güntherodt, P. Wachter, and D. M. Imboden, Phys. Condens. Mater. **12**, 292 (1971).

[5] J. Schoenes and P. Wachter, Phys. Rev. B **9**, 3097 (1974).

[6] K. Y. Ahn and M. W. Shafer, J. Appl. Phys. **41**, 1260 (1970).

[7] H.-Y. Wang, J. Schoenes, and E. Kaldis, Helv. Phys. Acta **59**, 102 (1986).

[8] R. Sutarto, S. G. Altendorf, B. Coloru, M. Moretti Sala, T. Haupricht, C. F. Chang, Z. Hu, C. Schüßler-Langeheine, N. Hollmann, H. Kierspel, J. A. Mydosh, H. H. Hsieh, H.-J. Lin, C. T. Chen, and L. H. Tjeng, Phys. Rev. B **80**, 085308 (2009).

[9] T. Mairoser, A. Schmehl, A. Melville, T. Heeg, L. Canella, P. Böni, W. Zander, J. Schubert, D. E. Shai, E. J. Monkman, K. M. Shen, D. G. Schlom, and J. Mannhart, Phys. Rev. Lett. **105**, 257206 (2010).

[10] H. Miyazaki, H. J. Im, K. Terashima, S. Yagi, M. Kato, K. Soda, T. Ito, and S. Kimura, Appl. Phys. Lett. **96**, 232503 (2010).

[11] J. B. Torrance, M. W. Shafer, and T. R. McGuire, Phys. Rev. Lett. **29**, 1168 (1972).

[12] Y. Shapira, S. Foner, and T. B. Reed, Phys. Rev. B **8**, 2299 (1973).

[13] G. M. Roesler Jr., M. E. Filipkowski, P. R. Broussard, Y. U. Idzerda, M. S. Osofsky, and R. J. Soulen Jr., in *Superconducting Superlattices and Multilayers*, edited by I. Bozovic (SPIE, Bellingham, 1994), Vol. 2517, pp. 285–290.

[14] M. Sohma, K. Kawaguchi, and Y. Oosawa, J. Appl. Phys. **81**, 5301 (1997).

[15] N. Iwata, G. Pindoria, T. Morishita, and K. Kohn, J. Phys. Soc. Jpn. **69**, 230 (2000).

[16] N. Iwata, T. Morishita, and K. Kohn, J. Phys. Soc. Jpn. **69**, 1745 (2000).

[17] P. G. Steeneken, Ph.D. thesis, Rijksuniversiteit Groningen, The Netherlands, 2002.

[18] P. G. Steeneken, L. H. Tjeng, I. Elfimov, G. A. Sawatzky, G. Ghiringhelli, N. B. Brookes, and D.-J. Huang, Phys. Rev. Lett. **88**, 047201 (2002).

[19] J. Lettieri, V. Vaithyanathan, S. K. Eah, J. Stephens, V. Sih, D. D. Awschalom, J. Levy, and D. G. Schlom, Appl. Phys. Lett. **83**, 975 (2003).

[20] T. Matsumoto, K. Yamaguchi, M. Yuri, K. Kawaguchi, N. Koshizaki, and K. Yamada, J. Phys. Condens. Matter. **16**, 6017 (2004).

[21] J. Holroyd, Y. U. Idzerda, and S. Stadler, J. Appl. Phys. **95**, 6571 (2004).

[22] T. S. Santos, and J. S. Moodera, Phys. Rev. B **69**, 241203 (2004).

[23] H. Ott, S. J. Heise, R. Sutarto, Z. Hu, C. F. Chang, H. H. Hsieh, H.-J. Lin, C. T. Chen, and L. H. Tjeng, Phys. Rev. B **73**, 094407 (2006).

[24] E. Negusse, J. Holroyd, M. Liberati, J. Dvorak, Y. U. Idzerda, T. S. Santos, J. S. Moodera, and E. Arenholz, J. Appl. Phys. **99**, 08E507 (2006).

[25] H. Lee, J.-Y. Kim, K.-J. Rho, B.-G. Park, and J.-H. Park, J. Appl. Phys. **102**, 053903 (2007).

[26]A. Schmehl, V. Vaithyanathan, A. Herrnberger, S. Thiel, C. Richter, M. Liberati, T. Heeg, M. Röckerath, L. F. Kourkoutis, S. Mühlbauer, P. Böni, D. A. Muller, Y. Barash, J. Schubert, Y. Idzerda, J. Mannhart, and D. G. Schlom, Nat. Mater. **6**, 882 (2007).
[27]S. Mühlbauer, P. Böni, R. Georgii, A. Schmehl, D. G. Schlom, and J. Mannhart, J. Phys. Condens. Matter **20**, 104230 (2008).
[28]G. van der Laan, E. Arenholz, A. Schmehl, and D. G. Schlom, Phys. Rev. Lett. **100**, 067403 (2008).
[29]R. W. Ulbricht, A. Schmehl, T. Heeg, J. Schubert, and D. G. Schlom, Appl. Phys. Lett. **93**, 102105 (2008).
[30]R. P. Panguluri, T. S. Santos, E. Negusse, J. Dvorak, Y. Idzerda, J. S. Moodera, and B. Nadgorny, Phys. Rev. B **78**, 125307 (2008).
[31]N. J. C. Ingle and I. S. Elfimov, Phys. Rev. B **77**, 121202 (2008).
[32]S.-I. Kimura, T. Ito, H. Miyazaki, T. Mizuno, T. Iizuka, and T. Takahashi, Phys. Rev. B **78**, 052409 (2008).
[33]H. Miyazaki, T. Ito, S. Ota, H. J. Im, S. Yagi, M. Kato, K. Soda, and S.-I. Kimura, Physica B: Condensed Matter **403**, 917 (2008).
[34]T. S. Santos, J. S. Moodera, K. V. Raman, E. Negusse, J. Holroyd, J. Dvorak, M. Liberati, Y. U. Idzerda, and E. Arenholz, Phys. Rev. Lett. **101**, 147201 (2008).
[35]S. M. Watson, T. S. Santos, J. A. Borchers, and J. S. Moodera, J. Appl. Phys. **103**, 07A719 (2008).
[36]R. Sutarto, S. G. Altendorf, B. Coloru, M. Moretti Sala, T. Haupricht, C. F. Chang, Z. Hu, C. Schüßler-Langeheine, N. Hollmann, H. Kierspel, H. H. Hsieh, H.-J. Lin, C. T. Chen, and L. H. Tjeng, Phys. Rev. B **79**, 205318 (2009).
[37]H. Miyazaki, T. Ito, H. J. Im, S. Yagi, M. Kato, K. Soda, and S. Kimura, Phys. Rev. Lett. **102**, 227203 (2009).
[38]E. Arenholz, A. Schmehl, D. G. Schlom, and G. van der Laan, J. Appl. Phys. **105**, 07E101 (2009).
[39]M. Müller, G.-X. Miao, and J. S. Moodera, J. Appl. Phys. **105**, 07C917 (2009).
[40]E. Negusse, J. Dvorak, J. S. Holroyd, M. Liberati,, T. S. Santos, J. S. Moodera, E. Arenholz, and Y. U. Idzerda, J. Appl. Phys. **105**, 07C930 (2009).
[41]M. Matsubara, A. Schmehl, J. Mannhart, D. G. Schlom, and M. Fiebig, Phys. Rev. B **81**, 214447 (2010).
[42]A. G. Swartz, J. Ciraldo, J. J. I. Wong, Yan Li, Wei Han, Tao Lin, S. Mack, J. Shi, D. D. Awschalom, and R. K. Kawakami, Appl. Phys. Lett. **97**, 112509 (2010).
[43]J. N. Beukers, J. E. Kleibeuker, G. Koster, D. H. A. Blank, G. Rijnders, H. Hilgenkamp, and A. Brinkman, Thin Solid Films **518**, 5173 (2010).
[44]T. Mairoser, A. Schmehl, A. Melville, T. Heeg, W. Zander, J. Schubert, D. E. Shai, E. J. Monkman, K. M. Shen, T. Z. Regier, D. G. Schlom, and J. Mannhart, Appl. Phys. Lett. **98**, 102110 (2011).
[45]D. F. Förster, J. Klinkhammer, C. Busse, S. G. Altendorf, T. Michely, Z. Hu, Y.-Y. Chin, L. H. Tjeng, J. Coraux, and D. Bourgault, Phys. Rev. B **83**, 045424 (2011).
[46]T. Yamasaki, K. Ueno, A. Tsukazaki, T. Fukumura, and M. Kawasaki, Appl. Phys. Lett. **98**, 082116 (2011).
[47]M. Barbagallo, N. D. M. Hine, J. F. K. Cooper, N.-J. Steinke, A. Ionescu, C. H. W. Barnes, C. J. Kinane, R. M. Dalgliesh, T. R. Charlton, and S. Langridge, Phys. Rev. B **81**, 235216 (2010).
[48]R. P. Ingel and D. Lewis III, J. Am. Ceram. Soc. **69**, 325 (1986).
[49]F. Lévy, Physik kondens. Mater. **10**, 71 (1969).
[50]V. R. PaiVerneker, A. N. Petelin, F. J. Crowne, and D. C. Nagle, Phys. Rev. B **40**, 8555 (1989).
[51]The reason for the shift of the MIT of the sample grown at 5.5×10^{-8} mbar oxygen pressure to lower temperatures is not known at the moment. We have the suspicion that it could be caused by an electrical contact problem of the thermometer.
[52]O. Massenet, Y. Capiomont, and N. Van Dang, J. Appl. Phys. **45**, 3593 (1974).
[53]J. C. Suits, K. Lee, H. F. Winters, P. B. P. Phipps, and D. F. Kyser, J. Appl. Phys. **42**, 1777 (1971).
[54]A. A. Samokhvalov, A. F. Gunichev, B. A. Gizhevskii, N. N. Loshkareva, N. M. Cebotaev, and N. A. Viglin, Sov. Phys. Solid State **20**, 519 (1978).
[55]A. S. Borukhovich, V. G. Bamburov, and A. A. Sidorov, J. Magn. Magn. Mater. **73**, 106 (1988).
[56]T. J. Konno, N. Ogawa, K. Wakoh, K. Sumiyama, and K. Suzuki, Jpn. J. Appl. Phys. **35**, 6052 (1996).
[57]A. J. Melmed, V. Maurice, O. Frank, and J. H. Block, J. Cryst. Growth **84**, 123 (1987).
[58]T. Gourieux, S. Fréchard, F. Dulot, J. Eugène, B. Kierren, and D. Malterre, Phys. Rev. B **62**, 7502 (2000).
[59]A. Mauger, Phys. Rev. B **27**, 2308 (1983).
[60]P. Sinjukow and W. Nolting, Phys. Rev. B **68**, 125107 (2003).